

Volatile Evolution in Thermoset Composites from Processing to Degradation

J.-D. Nam and J.C. Seferis¹

*Polymeric Composites Laboratory, Department of Chemical Engineering
University of Washington, Seattle, Washington 98195, USA*

CONTENTS

	Page
ABSTRACT	212
1. INTRODUCTION	212
2. EXPERIMENTAL	212
3. RESULTS AND DISCUSSION	213
A. Composite Cure Cycle from DSC Kinetic Analysis	213
B. Void Control in Consolidation Processing	217
C. TGA/FTIR Gas Analysis of Phenolic Resin Degradation	219
D. Thermal Characterization for High Temperature Processing	221
E. Composite Healing in High Temperature Processing	223
CONCLUSION	224
ACKNOWLEDGEMENT	224
REFERENCES	224

¹Author to whom correspondence should be addressed.

ABSTRACT

Using phenolic resin/carbon fiber composites as a model system, volatile evolution during thermoset composite processing was studied theoretically as well as experimentally. Water (and/or solvent) stabilization during the consolidation process could be described by combining gas-liquid phase equilibrium principles and the curing kinetics of the matrix system with a pseudo steady state approximation. Based on this consideration, voids from water (and/or solvents), which might vaporize during consolidation processing, could be suppressed by controlling the consolidation temperature and pressure with respect to time. Upon further heating the phenolic resin/carbon fiber composites up to 1000°C, composite degradation characteristics were investigated by using several thermal, mechanical, and chemical characterization techniques. Correlating these experimental results, characteristic features of each degradation stage were identified by weight loss, gas evolution, heat flow, dimensional stability, and modulus. Specifically, when the composite laminate was heated up to 300°C, where the matrix was expanding in the rubbery state, initially-generated microcracks were observed to close, resulting in a composite healing process.

1. INTRODUCTION

Carbon/carbon (c/c) composites are a superior structural material for extremely high temperature application because of their unique thermal, mechanical, and chemical properties. These composites are derived from conventional carbon fiber reinforced polymeric composites through high temperature pyrolytic processing. A specific structure of matrix-interface-fiber is developed during high temperature heat treatment processing, resulting in unique properties for the c/c composites /1-5/.

This matrix degradation processing, which is an essential step in c/c composite manufacturing, is considered to greatly affect the final performance and properties of c/c composites /1-7/. Specifically, the matrix, changing from organic polymer to inorganic carbon, with a reinforcing carbon fiber phase, is one of the major controlling factors in the processing and property characterization of c/c composites /8/. Therefore, it is necessary to clearly identify the processing characteristics related to structural development in order to control and meet specific performance characteristics of c/c

composites /9/.

Phenolic resin matrix systems have been utilized as matrix precursors for c/c composites because they are suitable for impregnation processes due to low viscosity. Also their char yield (about 60%) and char microstructure are considered most suitable for the required matrix characteristics of c/c systems /4/. However, it has been found that a considerable amount of shrinkage takes place (20% and 50% of linear and bulk shrinkage, respectively) during phenolic resin cure reaction, which is highly exothermic and generates water as a byproduct /10-12/. Thus, the lamination processing of phenolic resin/carbon fiber system is considered difficult and significant in controlling conventional lamination process parameters such as time, temperature, pressure, tooling, prepegging, lay-up and debulking, provided here as examples.

Accordingly, in this study, volatile evolution during composite processing was investigated with phenolic resin/carbon fiber composite as a model system. The consolidation heating cycle was determined by reaction kinetic studies made with a commercialized phenolic resin using a pressurized DSC thermal characterization technique. The volatilization of water produced by polymer condensation reactions was investigated kinetically and thermodynamically in order to identify processing conditions in terms of time, temperature, tooling and pressure. Finally, based on these considerations, void-formation mechanisms were experimentally investigated for various processing conditions.

Furthermore, high temperature processing was investigated at elevated temperatures up to 1000°C. Correlating several thermal characterization techniques, these degradation stages were analyzed to identify weight-loss and corresponding gas compositions, heat flow due to decomposition reactions, dimensional stability of the composite and viscoelastic modulus characteristics of the composite system during high temperature composite processing /9/.

Finally, composite healing and crack-propagation were found to occur in the first and second stages of the degradation, resulting from high temperature processing characteristics of phenolic resin/carbon fiber systems.

2. EXPERIMENTAL

In this study, a commercialized phenolic resin (SC-1008 manufactured by Borden Co.) was investigated as a model system for the kinetic

analysis. The physical properties of SC-1008 phenolic resin are shown in Table 1. The experiments were performed using a TA Instruments 910 pressure DSC. The sample sizes were 8 to 10 mg, and the samples were placed in a hermetic sealed aluminum pan. The pan was sealed and perforated at the top in order to improved the contact with the flowing nitrogen environment. Runs were always made using an empty pan as a reference.

Thermogravimetric measurements were performed with a TA Instruments 951 TGA interfaced to the TA Instruments 2000 Thermal Analyzer. SC-1008 phenolic resin was cured up to 325°F(162.8°C). The cured phenolic resin was pulverized to 80 Tyler mesh size, and samples were heated up to 1000°C in nitrogen at a flow rate of 100 ml/min. A Nicolet FTIR was connected to the TGA to analyze the evolved gases /13/. Modified GC/IR software was used to analyze the data.

Cured phenolic resin/carbon fiber composites were sliced less than 0.5 mm thick for DSC pyrolysis experiments. The resin content of the manufactured composites was measured as 40 wt% using an acid digestion method. The measurements were performed by a TA Instruments DSC 912 coupled to the TA Instruments 2000 Thermal Analyzer controller. The samples were heated at 5°C/min in flowing nitrogen.

The linear expansion of cured phenolic resin/carbon fiber composite was measured in the through-thickness direction using TA Instruments TMA 2940 coupled to the TA Instruments 2000 Thermal Analyzer controller.

The cured composite samples were also utilized for dynamic mechanical experiments. The experiments were carried out with a TA Instruments DMA 983 coupled to the TA Instruments 2000 Thermal Analyzer controller. Serrated clamps were used in the horizontal mode for a rectangular-shape composite sample whose dimensions were 15.32 x 4.59 x 0.95 mm. An oscillation amplitude was fixed at 0.1 mm, and the experiment was performed at a fixed frequency of 1 Hz. The samples were heated at 0.3°C/min in a nitrogen atmosphere.

The prepegs were T-300 8HS (eight-harness satin) weave carbon fiber cloth, provided by BF Goodrich Co. The physical properties of the prepeg are shown in Table 2. The laminates (8-12 plies) were cured in an autoclave (Lipton Steel & Metal Products, Inc.) with a controlled curing cycle, while full vacuum was applied from the beginning of the cure. Fig. 1 schematically shows a prepeg

lay-up showing a top- and bottom-bleeding system.

Debulking was carried out pressing the lay-ups between mold platens at 250 psi for 20 min at 77°C under vacuum. After cooling, the bagging was opened, old bleeder and breather cloths were replaced with new ones. Then, the bagging was resealed and evacuated. The debulked lay-ups were consolidated at 250 and 25 psig for comparison to non-debulk lay-ups.

3. RESULTS AND DISCUSSION

A. Composite Cure Cycle from DSC Kinetic Analysis

The condensation reactions are exothermic reactions, and therefore, thermoanalytical methods are particularly suited for the elucidation of thermal effects taking place during the curing reactions. Differential Scanning Calorimetry (DSC) is a valuable technique for investigating parameters associated with the curing or cross-linking reaction of thermosetting polymers /14/.

Assuming that the heat evolved in a small time interval is directly proportional to the number of moles reacting during that time, the degree of conversion, α , is defined as

$$\alpha = H_p / H_t \quad (1)$$

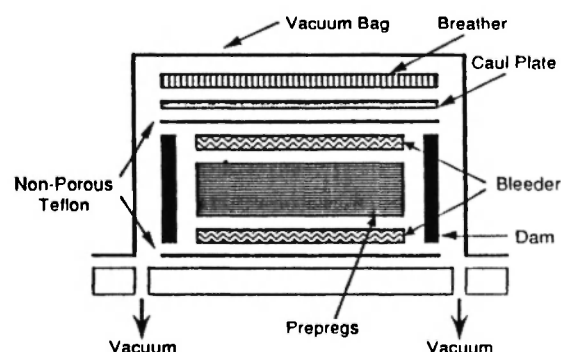


Fig. 1: Schematic representation of prepeg layup and bagging procedure for autoclave processing showing top- and bottom-bleeding system.

TABLE 1
PHYSICAL PROPERTY OF MODEL PHENOLIC RESIN

Property	Value
Appearance	clear amber liquid
pH, 25°C	7.8 - 8.5
Viscosity, Brookfield	180 - 300 cps
Flashpoint	80°F
Gel Time, G.E.	14 - 22 min @ 135°C
Solid, 135°C (vanishes)	60 - 64%
Specific Gravity, 25°C	1.070 - 1.100

TABLE 2
PROPERTY OF MODEL CARBON FIBER FABRI AND ITS PHENOLIC BASED PREPEG

Property	Value
Dry fabric weight	9.8335 oz/yd ²
Fiber density	1.902 g/cm ³
Dry fabric thickness	0.0195 in
Prepreg volatile content	10%
Resin solid	43%
Prepreg fiber areal weight	9.956 oz/yd ²
Resin flow	34%

where H_t is the total heat of reaction and H_p is taken as the partial area under the curve at time t . Then, the conversion rate can be obtained from the following equation:

$$\frac{d\alpha}{dt} = \frac{1}{H_t} \frac{dH}{dt} \quad (2)$$

where dH/dt is measured by the displacement of the curve exotherm from the baseline at time t .

If the reaction is assumed to follow n -th order kinetics, the following equation applies:

$$\frac{d\alpha}{dt} = k(T) (1-\alpha)^n \quad (3)$$

where α is the degree of conversion, $k(T)$ is the rate constant, and n is the order of reaction. The temperature dependence on the reaction rate may be expressed by an Arrhenius expression:

$$k(T) = A \exp (-E/RT) \quad (4)$$

where A is the pre-exponential factor, E is the activation energy, R is the gas constant, and T is absolute temperature.

For the kinetic analysis of SC-1008 phenolic resin, in this study, Borchardt-Daniels method was utilized, which is available as software in TA Instruments Thermal Analysis 2000 System /15/. According to this method, the reaction parameters, based on n -th order reaction, can be determined by a single constant-heating rate scan. Rearranging Eqs. 3 and 4 for two different temperatures, T_1 and T_2 , the following reaction is obtained

$$\frac{\ln[\alpha'_2 / \alpha'_1]}{\ln[(1-\alpha_2) / (1-\alpha_1)]} = - \frac{E}{R} \frac{1/T_2 - 1/T_1}{\ln[(1-\alpha_2) / (1-\alpha_1)]} + n \quad (5)$$

where $\alpha' = d\alpha/dt$. Subscripts 1 and 2 denote the values measured at T_1 and T_2 , respectively. As a result, by plotting the left-hand side of Eq. 5 vs $(1/T_2 - 1/T_1) / \ln[(1-\alpha_2) / (1-\alpha_1)]$, the activation energy and the reaction order are obtained from the slope and intercept of the resulting straight line. It must be the aim of any kinetic study to determine how a reaction proceeds. However, the determination of reliable kinetic data of a phenolic resin is complicated because the reaction conditions, including temperature, type and amount of catalyst, and mole ratios and polarity of the solvents, exert a profound influence on the result obtained. The purity of the raw materials, and even the nature of the reaction vessel, will play significant roles. The identification of the reaction products is also relatively difficult /16/. Therefore, it is not surprising that the reported kinetic data differ considerably.

The condensation reaction of phenolic resins occurring under normal atmospheric conditions leads to emission of volatile products, often water vapor, and this produces an endothermic peak which is large enough to obliterate the exotherm due to cross-linking. Condensation reactions therefore, requires encapsulation or pressurization if the curing exotherm is to be observed.

The pressurized system was first applied to phenolic resins by Ezrin and Claver /17/. Westwook investigated the kinetics of curing of base-catalyzed resol resin using sealed high-pressure DSC /18/. He reported an activation energy of 84.5 KJ/mole, reaction order of 1, and a heat of reaction of 263.7 KJ/mole for a Phenol (P)/Formaldehyde (F) molar ratio of 1:1.2. Kay, et

al. reported that the kinetic parameters of resol resin are not entirely independent of heating rate /19/. The activation energy range was obtained as 84.9 to 106.7 KJ/mole, and the reaction order was 1.0 ± 0.05 . Also the heat of reaction showed a higher value at a higher heating rate ranging between 267.4 and 318.0 J/g. The effect of P/F ratio on the heat of reaction was investigated by Erä, et al., where a linear correlation was reported between the heat of reaction and the P/F molar ratio /20/.

A typical pressurized DSC thermogram is compared with an ambient one in Fig. 2. In atmospheric conditions, it was noted that vaporization endotherms of monomers and water masked the curing exotherm. When the DSC cell was pressurized at 1000 psi and heated at a constant heating rate of $2^\circ\text{C}/\text{min}$ in a nitrogen atmosphere, an exothermic reaction peak could be obtained between 100°C and 200°C as shown in Fig. 2. In order to determine the kinetic parameters, a sigmoidal base line was used to consider the change in-heat capacity during the reaction. The heat of reaction, the area under the peak, was obtained as 233.4 J/g.

Using the pressure DSC, the kinetic parameters were determined by the Borchardt-Daniels method. Fig. 3 shows a linear relation in $\ln k(T)$ vs $1/T$ plot

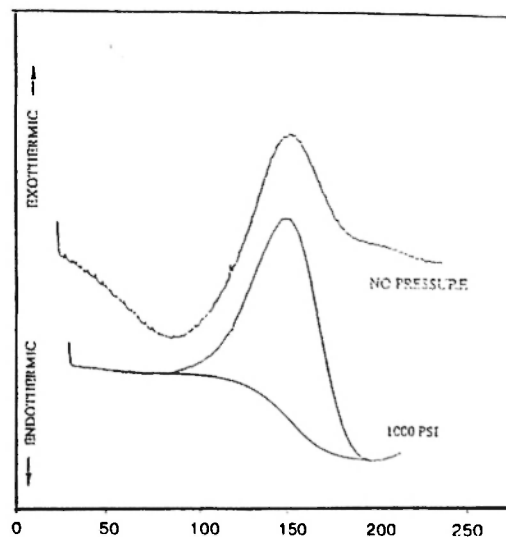


Fig. 2: Comparison of pressurized (1000 psi) and unpressurized DSC thermograms of SC-1008 phenolic resin at $2^\circ\text{C}/\text{min}$ heating rate.

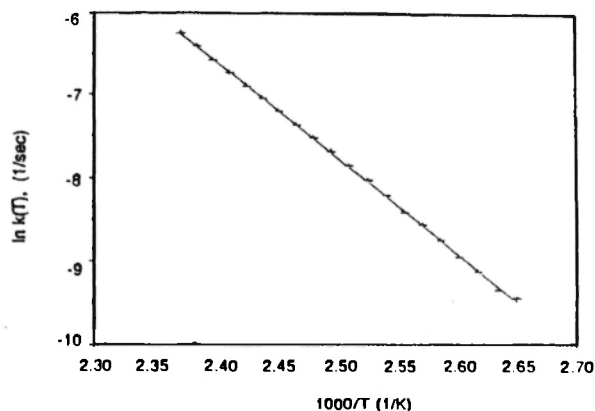


Fig. 3: Reaction constants obtained by Borchardt-Daniels kinetic method for SC-1008 phenolic resin. Activation energy is calculated from the slope as 96.1 kJ/mol with $n=1.37$ and $\log(A) = 10.96$.

with a reaction order of 1.37. The slope gives the activation energy of 96.1 KJ/mole, and finally the pre-exponential factor of $10^{10.96} \text{ min}^{-1}$. As shown in Figures 4 and 5, these kinetic parameters were used for the estimation of isothermal conversion as a function of time and temperature. In particular, three temperatures of 200, 250 and 325°F (93.3, 121.1, and 162.8°C, respectively) were chosen in Fig. 4, because they could be used in designing a

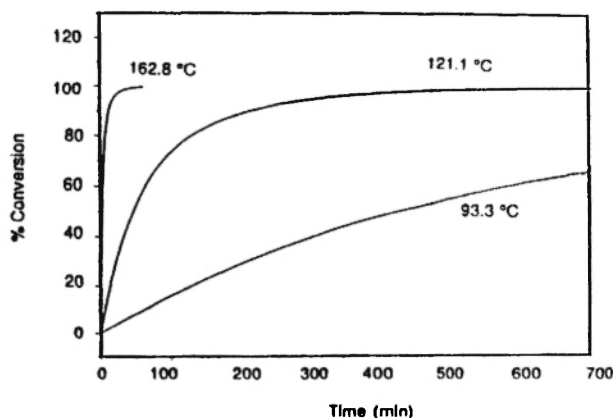


Fig. 4: Predicted isothermal conversion as a function of time at different temperatures for SC-1008 phenolic resin.

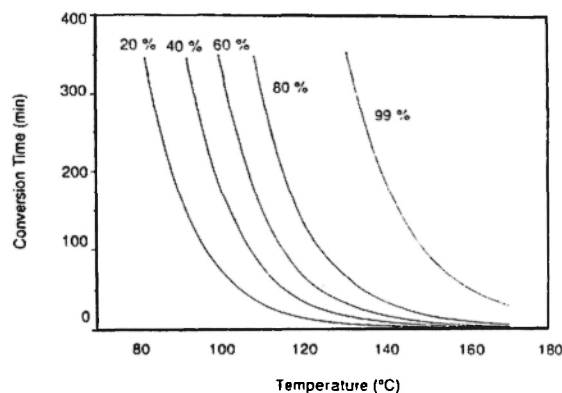


Fig. 5: Predicted conversion time as a function of time for various SC-1008 phenolic resin conversion levels.

cure cycle for the system. In order to increase the mobility of the resin and control the resin content in the fiber bundles before curing, the first isothermal holding temperature was specified as 200°F. The main reaction might take place between 200°F and 250°F with a controlled heating rate, which must be slow enough to release the energy produced by the highly exothermic heat of reaction. The curing reaction may be assumed to be complete when the curing temperature reaches 325°F.

Accordingly, a proposed curing cycle is summarized below:

1. Room temperature to 200°F (93.3°C) in 30 min
2. 200°F (93.3°C) hold for 1 hr.
3. 200°F (93.3°C) to 250°F (121.1°C) in 1 hr.
4. 250°F (121.1°C) to 325°F (162.8°C) in 1 hr.
5. 325°F (162.8°C) hold for 1 hr.

Using the above heating cycle, Eqs. 3 and 4 were solved for the degree of conversion by using a RKF45 package which is based on the Runge-Kutter-Feldberg formulas [12]. The degree of conversion is plotted in Fig. 6 as a function of time for the specified curing cycle. The reaction seems to take place between 250 and 325°F slowly, while it reaches completion shortly after 325°F. In a large scale manufacturing process, however, heat transfer effects including heat of vaporization, and tooling on the curing process, as well as vacuum and/or pressure application should also be

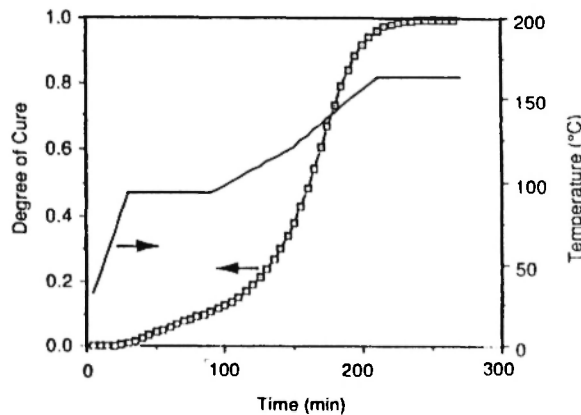


Fig. 6: Degree of conversion prediction of SC-1008 phenolic resin as a function of processing time for the proposed curing cycle.

considered. Thus, the proposed curing cycle might be different in large scale processing.

B. Void Control in Consolidation Processing

The void-formation mechanism of high performance structural composite laminates basically lacks a firm scientific basis. Voids are considered to be formed by entrapment of humid air, of which water content depends on the humidity of the factory environment, or by nucleation processes. Kardos, et al. reviewed the void phenomena in terms of its nucleation, growth and transport during autoclave laminate processing /22/. Correlating thermodynamic and molecular-diffusion theories, the void-formation mechanism was practically investigated in relation to the humidity of the lay-up environment by Halpin, et al. /23/. Modeling of void size and pressure inside the void was also performed considering the diffusion of vapor molecules into the voids /24/. However, these void formation models have not been verified by experiments not only because the material properties in the model equations are difficult to measure, but also more complex void-related mechanisms may take place due to heterogeneous and anisotropic fiber reinforcement.

When humid air is entrapped during lay-up, air-including voids are formed and are not likely to be dissolved into the resin because the solubility of air in the resin is limited. In this case, the debulking

process under vacuum is likely to be effective to minimize the void formation in the final product. The size of the air voids can be minimized by the applied pressure during consolidation.

In addition, void formation may also take place when water and/or solvents present in the system are superheated during consolidation. Water is a by-product of condensation reactions and solvents are present if the prepegs are prepared by solvent-assisted impregnation. These voids can be controlled by temperature and pressure processing conditions. If the curing temperature is kept lower than the boiling point of water or of the solvents during cure, they will remain dissolved in the resin. Thus, if the consolidation pressure is higher than the saturated pressure of water or solvents, they will be kept dissolved in the resin. The gas-liquid equilibrium can be described by Raoult's law for an ideal-gas and ideal-solution mixture /25/:

$$y_i P = x_i P_i^{\text{sat}}(T) \quad (6)$$

where P is the pressure, x_i and y_i are the mole fraction of a component i in the liquid and gas phase, respectively, and $P_i^{\text{sat}}(T)$ is the saturation pressure of pure liquid i at a temperature T . The component i designates water or solvents of interest in the vapor-induced lamination process.

If vaporization of resin is assumed negligible during consolidation, $y_i \approx 1.0$, then the boiling temperature of a component at a certain pressure may be described:

$$P \approx x_i P_i^{\text{sat}}(T) \quad (7)$$

The saturation pressure can be described by the Clausius-Clapeyron equation with two parameters /25/:

$$\log P^{\text{sat}} = A - \frac{B}{T} \quad (8)$$

where $A=7.0023$ and $B=2181.4$ for water. T is expressed in Kelvin degrees.

As a result, the boiling temperature of water (or

solvents) depends on the resin pressure and the mole fraction of water (or solvents) in the resin. During the consolidation process, at each temperature and pressure, pseudo steady state may be established with respect to the mole fraction, which changes with conversion that is basically a kinetic variable.

For the formation of an ideal structure of phenolic resin, 1.0 mole of phenol (P) may be assumed to react with 1.5 mole of formaldehyde (F) to form a methylene bridge, producing 1.5 mole of water and 1.0 mole of F-P compound. If the reactant molar ratio of F/P is assumed as 1.5 (which may not be a practical formulation of commercial resin systems, but sufficient to illustrate our point), the mole fraction of water in the resin can be described as a function of conversion:

$$x_i = \frac{0.5 \alpha}{2.5 + 0.5 \alpha} \quad (9)$$

where α is the degree of cure defined by Eq. 1.

If the determined reaction kinetics are combined with Eqs. (7)-(9) under the pseudo steady state assumption, we can estimate the resin pressure required to suppress the vaporization of water at a certain temperature during the consolidation process. From Table 1, the gel time of SC-1008 phenolic resin was specified as 14-22 min at 135°C. This time and temperature correspond to a gel conversion of 0.43-0.57 calculated by the reaction kinetics determined by DSC. As a result, the resin pressure should be kept high enough to suppress the vaporization of water up to 43-57% of conversion in the processing.

In order to compare the boiling temperature and the processing temperature cycle, two consolidation conditions were examined: Pressure was increased to 25 psi (cycle 1) and 250 psi (cycle 2) in 1 hour, and was held constant at that pressure. These two pressure cycles as well as the temperature cure cycle are shown in Fig. 7. It has been experimentally determined that only 5-10% of consolidation pressure is effectively applied to the resin, while the rest is shared with the fiber network [26,27]. In this study, 5% of the consolidation pressure was assumed to be applied to the resin.

Accordingly, the determined heating cycle was utilized to calculate the saturated pressure and mole fraction of water during cure reaction using Eqs. (8) and (9), resulting in equilibrium pressure

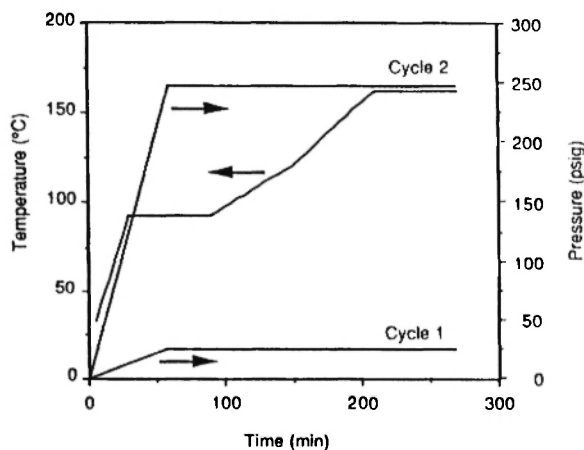


Fig. 7: Temperature and pressure consolidation conditions for phenolic resin composites denoted by cycle 1 and cycle 2 for 25 and 250 psig, respectively.

from Eq. (7). This temperature-pressure relation is represented by the boiling curve in Fig. 8. Also, the same temperature cycle as the boiling curve and the two different pressure cycles give temperature-pressure relationships denoted by cycle 1 and 2 in Fig. 8. As can be seen in this

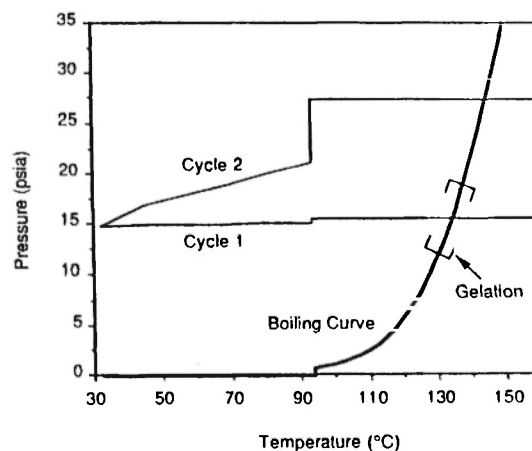


Fig. 8: Comparison of water boiling curve and two processing cycles with different consolidation conditions. Consolidation pressures for cycle 1 and 2 are 25 psig and 250 psig, respectively.

figure, cycle 1 crosses the water boiling curve possibly during gelation of the resin. Therefore, the water produced by condensation reactions may vaporize and produce voids because the resin is still in a liquid state before gelation. On the other hand, cycle 2 does not cross the boiling curve before the resin gelation. The vaporization of produced water seems to be suppressed because the resin pressure during gelation is higher than the water vapor pressure. Thus, no voids are expected to form during this consolidation process.

Based on this qualitative consideration, the void formation mechanism was experimentally investigated during composite fabrication processing of the model composite system that consisted of phenolic resin/carbon fiber. Two processing conditions were chosen to observe void formation mechanisms: debulking and consolidation pressure. The debulking process was considered to be related to mechanically entrapped voids during lay-up processing. However, the consolidation pressure was likely to affect the vaporization of water and/or solvent to form voids.

Fig. 9a shows optical microscope pictures of a composite consolidated at 250 psi without debulking. As can be seen, large entrapped pores are observed between the prepeg layers. The voids seem to be mechanically entrapped during lay-up processing because they are observed only between the layers and their size is non-uniform and quite large. On the other hand, when the composite laminates were first debulked and then consolidated at 25 psi, optical micrographs as seen in Fig. 9b exhibited small voids generated in the fiber bundle all over the composite cross section. These voids are clearly distinguished from those in Fig. 9a in terms of their size and position. The consolidation pressure, 25 psi, seems to be too small to suppress water vaporization as presented by cycle 1 in Fig. 8. Finally, composite laminates were debulked and consolidated at 250 psi, and a cross section of the composite is shown in Fig. 9c. No voids were observed neither inside nor between the layers. These results implied that the mechanically entrapped voids may be removed by the debulking process and water produced by condensation reactions may be suppressed by an increased consolidation pressure, as specified by cycle 2 in Fig. 8.

C. TGA/FTIR Gas Analysis of Phenolic Resin Degradation

Fig. 10a shows the Gram-Schmidt reconstruction curve representing four peaks that were attributed

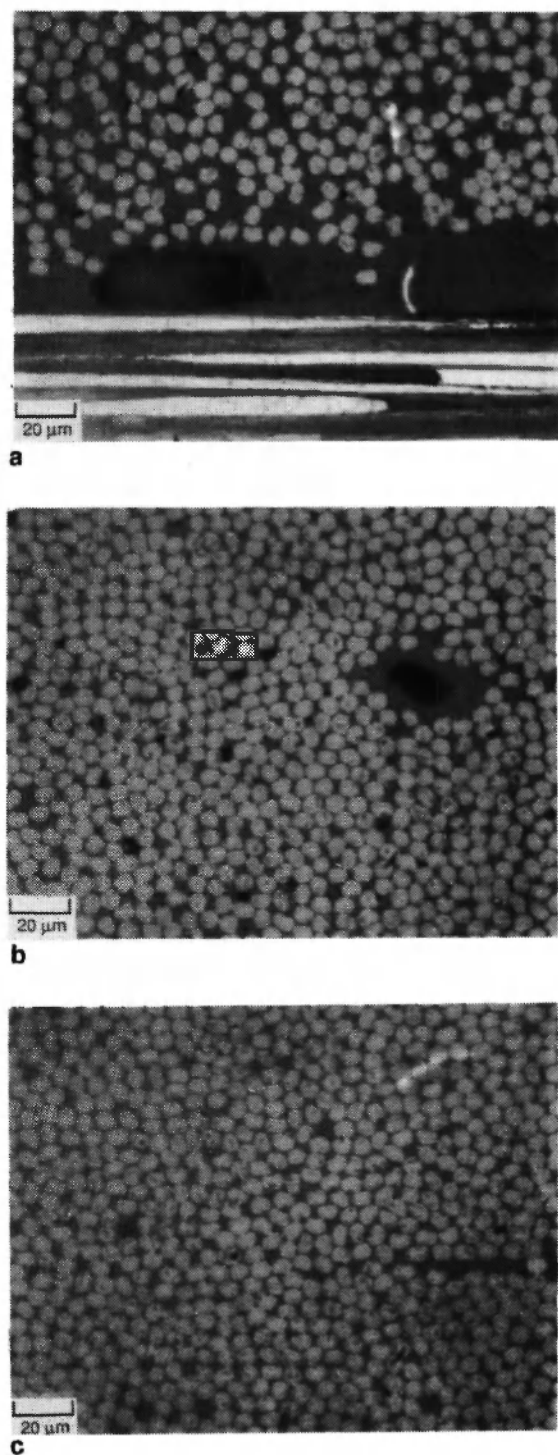


Fig. 9: Optical micrograph of phenolic resin/carbon fiber composite manufactured (a) at 250 psi consolidation pressure without debulking process, (b) at 25 psi consolidation pressure with debulking process, and (c) at 250 psi consolidation pressure with debulking process.

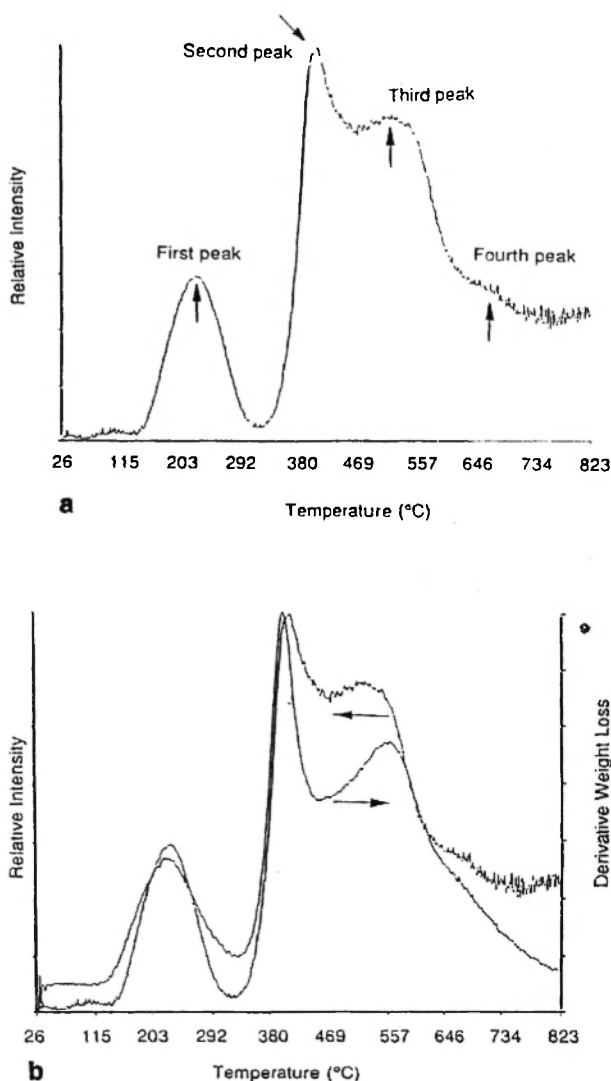


Fig. 10: Gram-Schmidt reconstruction curve for cured SC-1008 phenolic resin (a) representing different gas compositions by four peaks, and (b) compared with derivative weight loss.

to different gas compositions during degradation of the cured phenolic resin /28-30/. In this figure, ten basic vectors were taken at the beginning of the TGA/FTIR experiment in order to obtain stronger signal intensity with respect to the base line by suppressing the undesired features. The basic set then described the initial conditions when only carrier gas was flowing through the TGA/FTIR. When interferogram segments from each of the interferograms in the run were obtained and projected on the basic set, each point of Gram-

Schmidt reconstruction could be calculated in the computer.

The reconstruction curve was compared with the first derivative of the weight loss curve in Fig. 10b. The peak positions of both curves coincide with each other but the fourth peak is better represented by the Gram-Schmidt reconstruction. Even though the SC-1008 is a commercialized phenolic resin, the weight loss behavior is favorably comparable with the results reported in the literature /10, 31/.

Each peak of the reconstruction, represented in Fig. 10a, was analyzed and the IR spectrum associated with each peak is shown in Figs. 11a-11d. Fig. 11a shows the FTIR spectrum of the first stage of weight loss, and the evolved gases turn out to be CO_2 , phenol groups (cresols), and water, which demonstrate that the condensation reaction is taking place up to 330°C. Phenol is likely to be the entrapped monomer uncured in the low temperature curing, and water is produced by the reactions between $-\text{CH}_2\text{OH}$ and the aromatic hydrogen /32/.

Fig. 11b shows that water and phenol group gases are the main evolution of products in the second stage of degradation between 330°C and 450°C. Evolution of water can be attributed to a de-watering process, which may be regarded as mainly a postcuring reaction between the hydroxyl and methylene group and also between the two hydroxyl groups by which the network structure is developed /32/. During this degradation stage, random chain scission is also known to occur. Therefore, compounds with phenol groups may be the by-products from chain scission reactions.

As shown in Fig. 11c, CH_4 , CO , and CO_2 , as well as phenol groups, appear in the third stage of degradation between 450°C and 600°C. CH_4 may be formed from methylene groups which do not participate in dehydration reactions. CO is known to be produced from decomposition of ether bonds. Accordingly, the generation of CO and CH_4 may be ascribed to the char formation process /32-37/.

As degradation continues, phenol and CO_2 disappear as can be seen in Fig. 11d, but CH_4 and CO are still being generated in a temperature range over 650°C. Conclusively, char formation reaction producing CO and CH_4 is likely to take place in this weight loss stage. Even though H_2 cannot be detected in the FTIR, dehydration reactions are likely to continue to occur in this stage.

In conclusion, the evolved gas analysis by the TGA/FTIR on-line experiment provided information to postulate high temperature reaction

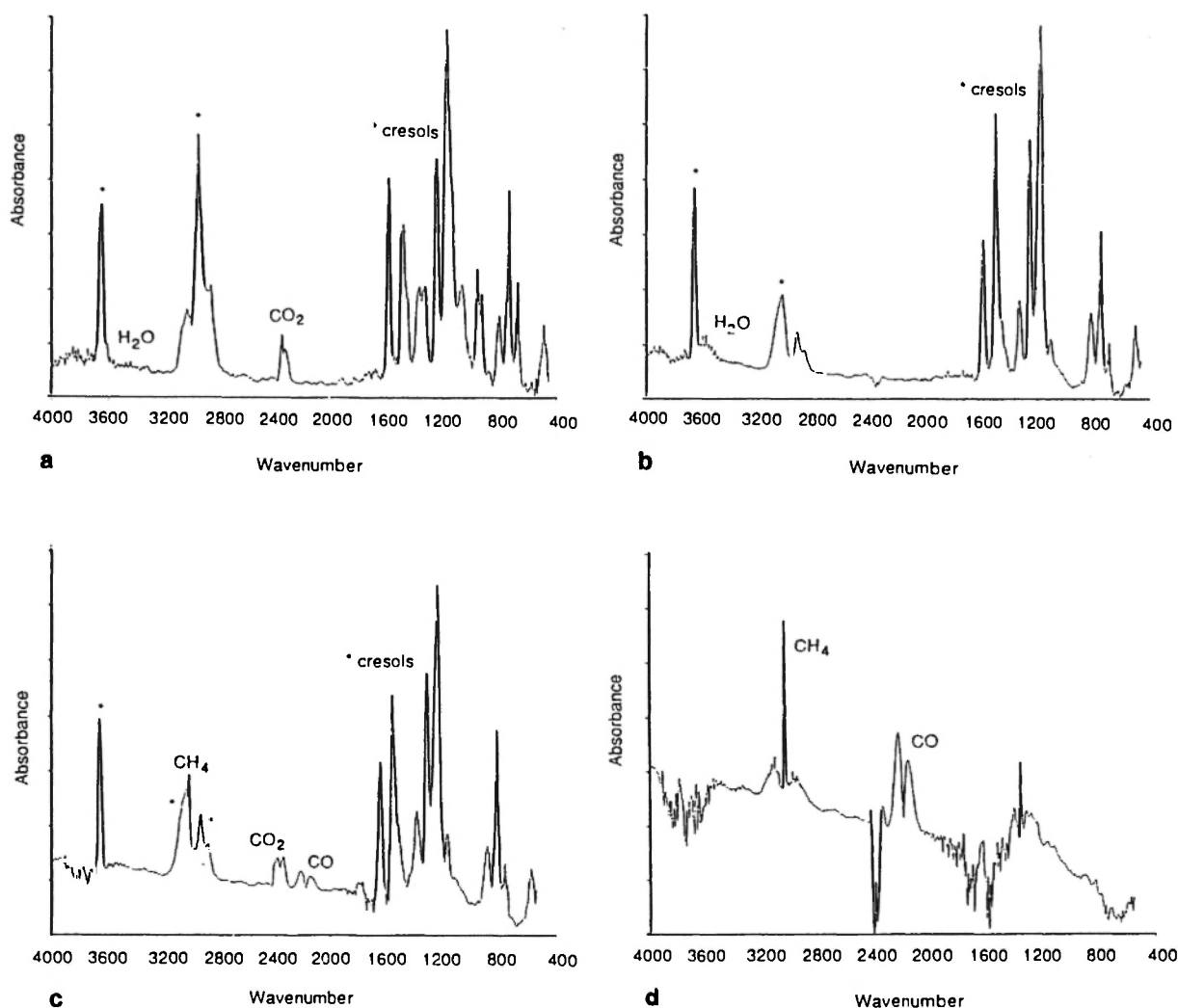


Fig. 11: FTIR spectrum of cured SC-1008 phenolic resin at the peaks of Gram-Schmidt reconstruction curve: (a) first peak, (b) second peak, (c) third peak, and (d) fourth peak.

mechanisms in a continuous fashion. For instance, the postcuring reaction was detected by water evolution, and the char formation reaction could be elucidated in a high temperature range by the generation of CO and CH₄. The degradation of commercialized phenolic resin system, SC-1008, used in this study, was favorably compared with the results reported in the literature, showing low temperature curing, postcuring, chain scission, and char formation reactions.

D. Thermal Characterization for High Temperature Processing

Fig. 12 shows the weight loss and its derivative curve obtained at 5°C/min heating rate for the

postcured phenolic resin at 250°C for 15 hours. Three peaks of the derivative weight loss curve can be seen at 300°C, 400°C and 538°C. As was observed in the FTIR analysis, the first peak may be attributed to the low-temperature condensation reaction and vaporization of unreacted monomers. The second peak is ascribed to the high-temperature crosslinking and random chain scission reactions simultaneously taking place. The third peak seems to be the char formation reactions and oxidation reactions initiated by water and/or ether bonds. The fourth stage of degradation is not clearly seen in the TGA results, which has been observed better in the Gram-Schmidt reconstruction curve. These peak temperatures representing each degradation stage were found to correlate well with the thermal characteristics of

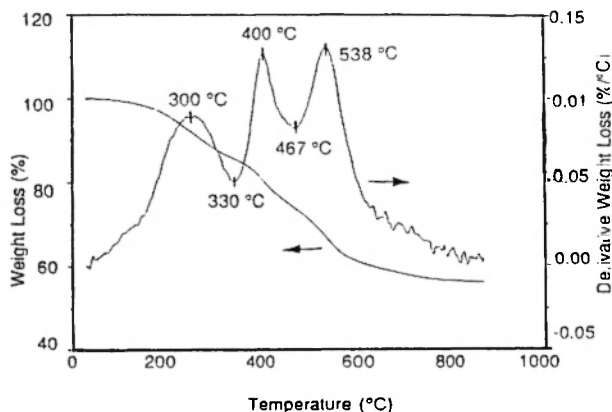


Fig. 12: TGA weight loss and its derivative curves of cured SC-1008 phenolic resin at 5°C/min heating rate in nitrogen atmosphere.

the material.

Specifically DSC results shown in Fig. 13 exhibit a degradation endotherm of the phenolic resin composite between 150°C and 650°C. The heat of reaction was estimated as 234.0 J/g. The three stages of degradation, observed in TGA and FTIR experiments, are not distinguished in the DSC endotherm, but the fourth degradation stage was clearly seen around 600°C.

Fig. 14 shows the TMA thermograms generated at 5°C/min and 50°C/min in nitrogen atmosphere. In the 5°C/min experiment, the composite expands up to 403°C, which corresponds to the second

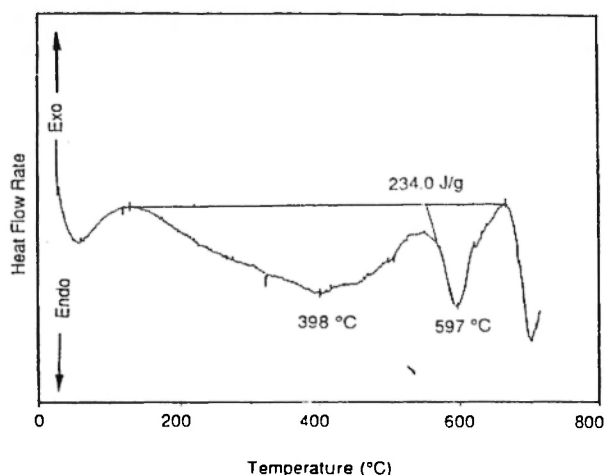


Fig. 13: DSC thermogram of cured SC-1008 phenolic resin/carbon fiber composite at 5°C/min heating rate nitrogen atmosphere.

stage of degradation, and then decreases in the temperature range between 403°C and 582°C, which can be ascribed to the third stage of degradation. After these degradation stages of major weight loss, the composite continues to expand throughout the fourth degradation stage. The first and second stages of degradation can be distinguished by an inflection point at a fast heating rate of 50°C/min.

Fig. 15 shows the DMA moduli of phenolic resin/carbon composite illustrating a constant storage modulus for the glass state up to 220°C. The major modulus drop is observed between 230°C and 300°C, which corresponds to the first degradation stage. This degradation stage is likely to be overlapped with the glass transition of the curing phenolic resin represented by the decreasing modulus. The rubbery state of composite is observed between 300°C and 320°C, where the composite is relaxed and easy to deform to some extent. As found in the TMA experiments, the composite continues to expand in this temperature range. Therefore, there may be significant mobility of the matrix material in a micro- as well as a macro-scale. Passing the rubbery modulus, the composite becomes stiffer and stiffer up to 400°C, which is ascribed to the second stage of degradation. These two transitions, ascribed to the first and second degradation stages, are well represented by two peaks in G'' and $\tan \delta$ curves.

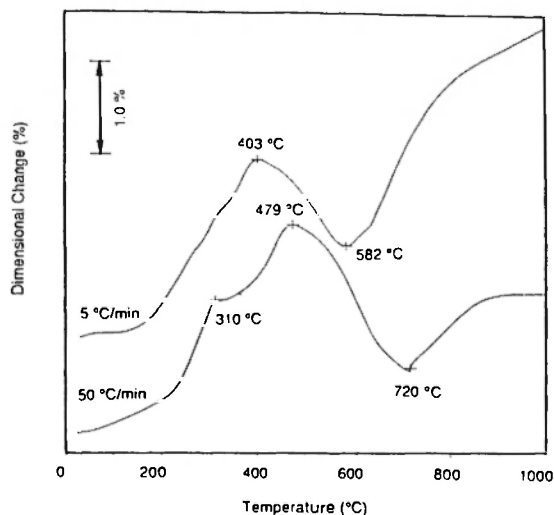


Fig. 14: Through-thickness linear expansion of cured SC-1008 phenolic resin/carbon fiber composite measured by TMA at 5°C/min and 50°C/min heating rates in nitrogen atmosphere.

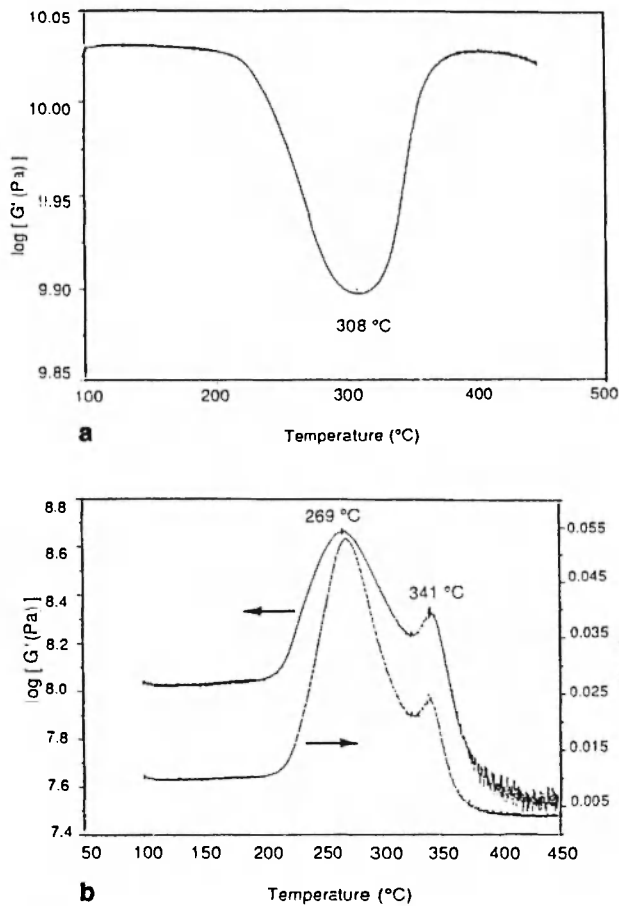


Fig. 15: Dynamic mechanical measurements of cured SC-1008 phenolic resin/carbon fiber composite at 0.3 $^{\circ}\text{C}/\text{min}$ heating rate in nitrogen atmosphere: (a) shear storage modulus, and (b) shear loss modulus and $\tan \delta$ curves.

E. Composite Healing in High Temperature Processing

It is well known that there is considerable shrinkage of phenolic resin during curing, which is reported as 50% based on volume [11]. This shrinkage often results in microcracks in the curing resin. Fig. 16a shows a cross section of a cured phenolic resin/carbon fiber composite. Many microcracks are clearly seen running in the through-thickness direction of the composite, seemingly due to the resin shrinkage.

As a result of thermal characterization, it was found that 300 $^{\circ}\text{C}$ is an important point in high temperature processing because the matrix expands and its mobility is enhanced. Therefore, in

manufacturing of c/c composites, the part may have to be held at this temperature for a period of time in order to release internal stresses. Fig. 16b demonstrates the composite healing effect, which has been inferred by the thermal characterization

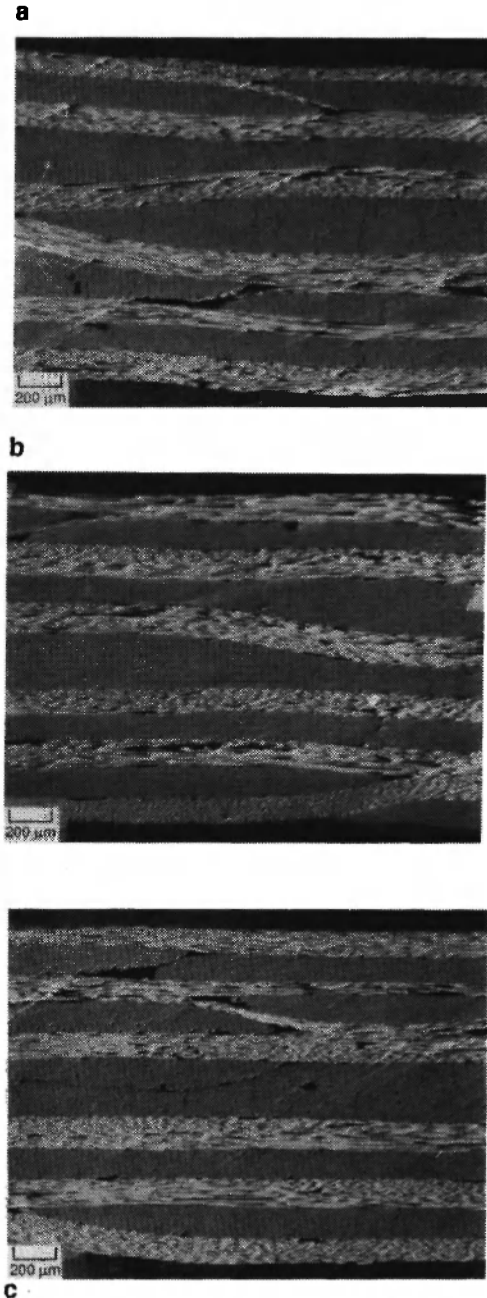


Fig. 16: Optical micrograph of phenolic resin/carbon fiber composite (a) cured to 162.8 $^{\circ}\text{C}$ (325 $^{\circ}\text{F}$) without high temperature heat treatment, (b) heated up to 300 $^{\circ}\text{C}$ at 5 $^{\circ}\text{C}/\text{min}$ in nitrogen atmosphere, and (c) heated up to 410 $^{\circ}\text{C}$ at 5 $^{\circ}\text{C}/\text{min}$ in nitrogen atmosphere.

results. As can be seen, when the composite is heated to 300°C at 5°C/min, the cracks initially developed are healed and have disappeared. It can be physically interpreted that cracks in the rubbery matrix are pressed by the expanding feature of the matrix characteristics, resulting in crack healing.

Upon further heating the composite to 410°C, microcracks begin to propagate again both in the through-thickness and in-plane directions, as can be seen in Fig. 16c. As found in the thermal characterization experiments, the matrix modulus increases, and the composite loses a large amount of matrix in this stage of degradation. Accordingly, the matrix seems to be stiff and insufficient to hold fibers together at this stage of degradation.

4. CONCLUSION

Carbon/carbon composites are derived from conventional polymeric composites through high temperature processing. Therefore, this study began from the fundamentals of thermoset-based composite processing. Due to the vaporization of solvents and/or water produced during cure, a phenolic resin matrix system was investigated as a model system for volatile evolution in composite processing. Using a pressurized DSC characterization technique, the curing kinetics of a commercialized phenolic resin (SC-1008) were determined. Based on this kinetic analysis, a composite cure cycle was developed.

Focusing on the water volatilization during consolidation processing, the void-formation mechanism was studied combining the cure kinetics and phase equilibrium thermodynamic principles based upon a pseudo steady-state assumption. A water boiling curve was obtained from the determined temperature cure cycle in a temperature-pressure plot, and it was compared with several consolidation pressure conditions. This qualitative analysis demonstrated the importance of the consolidation time-temperature-pressure cycle in void-formation control.

Validating the theoretical considerations, the void formation mechanisms were experimentally investigated, and two different types of voids were found to occur during the consolidation process: mechanically entrapped voids and vaporized voids from water (and/or solvent). Understanding the void formation mechanisms, a void-free composite was successfully manufactured by controlling the consolidation processing conditions: (1) the

consolidation pressure and (2) the debulking process.

Combining thermal, mechanical and chemical characterization techniques, high temperature composite processing was also investigated in this study. Analyzing the decomposed gases of cured phenolic resin matrix by TGA/FTIR on-line experiments, the degradation mechanism was clearly identified and correlated with the weight-loss characteristics. The four stages of composite degradation were also investigated by heat flow (DSC), dimensional change (TMA) and modulus change (DMA). As a result, the first stage of degradation was considered a composite healing stage because the matrix is rubbery and expanding to close microcracks in the composite. The second stage of degradation was likely to be a crack-propagating stage of high temperature processing because the matrix lost a considerable amount of resin and its modulus was increased.

Collectively then, this study provided an integration of experimental and analytical techniques which formed the foundation for analyzing volatile evolution found in thermoset composites from the processing step to degradation. Although viewed as separate steps in traditional composite structures, they must be integrated for understanding carbon/carbon composite processing.

ACKNOWLEDGEMENT

The authors would like to express their appreciation to Dr. David C. Bonner, Mr. Larry D. Benson and Mr. William H. Pfeifer of the BF Goodrich Company for helpful discussions and identification of the problem. Financial assistance for this work was provided by the BF Goodrich Company through project support to the Polymeric Composites Laboratory at the University of Washington.

REFERENCES

1. Fitzer, E., Gkogkidis, A. and Heine, M., *High Temperatures-High Pressures*, **16**, 363 (1984).
2. Fitzer, E., *Carbon*, **25**, 163 (1987).
3. Buckley, J.D., *Ceramic Bulletin*, **67**, No. 2, 364 (1988).
4. McAllister, L.E. and Lachman, W.L., "Multidirectional Carbon-Carbon Composites: Handbook of Composites", A.

- Kelly and Y.N. Rabotnov, Eds., Elsevier Science Publishers, New York (1983).
5. Brahney, J.H., *Aerospace Engineering*, June, 11 (1987).
6. Kowbel, W. and Shan, C.H., *Carbon*, **28**, 127 (1991).
7. Chlopek, J. and Bizewicz, S., *Carbon*, **29**, 127 (1991).
8. Nam, J.D. and Seferis, J.C., *Carbon*, submitted (1991).
9. Nam, J.D., Ph.D. Dissertation, Department of Chemical Engineering, University of Washington (1991).
10. Knop, A. and Pilato, L.A., "Phenolic Resins", New York, Springer-Verlag (1985).
11. Fitzer, E., Schaefer, W. and Yamada, S., *Carbon*, **7**, 643 (1969).
12. Brydson, J.A., "Plastics Materials", 5th Ed., Butterworths, Boston (1989).
13. Lewis, M.L., Nam, J.D., Seferis, J.C. and Prime, R.B., Proc. Soc. Plast. Eng. 47th ANTEC '89 Conf., New York, 1092 (1989).
14. Turi, E.A., "Thermal Characterization of Polymeric Materials", New York, Academic Press (1981).
15. Borchardt, H.J. and Daniels, F., J. Am. Chem. Soc., **79**, 41 (1957).
16. Megson, N.J.L., "Phenolic Resin Chemistry", London, Butterworths (1975).
17. Ezrin, M. and Claver, G.C., *Appl. Polym. Symp.*, **8**, 159 (1969).
18. Westhook, A.R., Thermal Analysis Proc. of the 3rd ICTA, Davos, **3**, 169 (1971).
19. Kay, P. and Westhook, A.R., *Eur. Polym. J.*, **11**, 25 (1975).
20. Erä, V., Lindberg, J.J., Mattila, A., Vaukonen and Linnahalme, T., *Angew. Makromol. Chem.*, **46**, 187 (1975).
21. Forsythe, G., Malcolm, M. and Moler, C., "Computer Methods for Mathematical Computation", Prentice-Hall, Englewood Cliffs, N.J. (1977).
22. Kardos, J.L., Dudukovic, M.P., McKague, E.L. and Lehman, M.W., "Composite Materials: Quality Assurance and Processing", ASTM STP 797, C.E. Browning, Ed., American Society for Testing and Materials, pp. 96 (1983).
23. Halpin, J.C., Kardos, J.L. and Dudukovic, M.P., *Pure & Appl. Chem.*, **55**, No. 5., 893 (1983).
24. Loos, A.C. and Springer, G.S., *J. Comp. Mat.*, **17**, 135 (1983).
25. Prausnitz, J.M., Lichtenthaler, R.N. and de Azevedo, E.G., "Molecular Thermodynamics of Fluid-Phase Equilibria", Prentice Hall Inc., Englewood Cliff, N.J. (1986).
26. Gutowski, T.G., Cai, Z., Baner, S., Boucher, D., Kingery, J. and Wineman, S., *J. Comp. Mat.*, **21**, 650 (1987).
27. Gutowski, T.G., Cai, Z., Kingery, J. and Wineman, S., *SAMPE Quarterly*, **17**, 54 (1986).
28. de Haseth, J.A. and Isenhour, T.L., *Anal. Chem.*, **4**, 1977 (1977).
29. Weiboldt, R.C. and Hanna, D.A., *Anal. Chem.*, **59**, 1255 (1987).
30. Strang, G., "Linear Algebra and Its Application", Academic, New York (1976).
31. Jackson, W.M. and Conley, R.T., *J. of Appl. Polym. Sci.*, **8**, 2163 (1964).
32. Yamashita, Y. and Ouchi, K., *Carbon*, **19**, 89 (1981).
33. Yamashita, Y. and Ouchi, K., *J. Fuel Soc. Japan*, **53**, 1064 (1974).
34. Conley, R.T., *J. of Appl. Polym. Sci.*, **9**, 1117 (1965).
35. Conley, R.T. and Bieron, J.F., *J. of Appl. Polym. Sci.*, **7**, 103 (1963).
36. Conley, R.T., "Thermal Stability of Polymers", New York, Mercel Dekker Inc. (1970).
37. Lochte, H.W., Strauss, E.L. and Conley, R.T., *J. of Appl. Polym. Sci.*, **9**, 2799 (1965).